

DR. JULIA VON FROWEIN (Orcid ID : 0000-0001-5522-2805)

Article type : Original Articles

Handling Editor: Frank Tacke

MiR-492 regulates metastatic properties of hepatoblastoma via CD44

Julia von Frowein¹, Stefanie M. Hauck², Roland Kappler³, Philipp Pagel^{4,5}, Katrin K. Fleischmann¹,
Thomas Magg¹, Stefano Cairo^{6,7}, Adelbert Roscher⁸, Dietrich von Schweinitz³, Irene Schmid¹

¹Children's Research Center, Department of Pediatric Hematology and Oncology, Dr. von Hauner Children's Hospital, Ludwig-Maximilians-University Munich, Germany

²Research Unit Protein Science, Helmholtz Zentrum Munich (GmbH), German Research Center for Environmental Health, Germany

³Department of Pediatric Surgery, Dr. von Hauner Children's Hospital, Ludwig-Maximilians-University Munich, Germany

⁴Lehrstuhl für Genomorientierte Bioinformatik, Technische Universität München, Freising, Germany

⁵numares AG, Regensburg, Germany

⁶University of Ferrara, Department of Morphology, Surgery and Experimental Medicine, Ferrara, Italy

This article has been accepted for publication and undergone full peer review but has not been through the copyediting, typesetting, pagination and proofreading process, which may lead to differences between this version and the Version of Record. Please cite this article as doi:

10.1111/liv.13687

This article is protected by copyright. All rights reserved.

⁷XenTech, Evry, France

⁸Children's Research Center, Dr. von Hauner Children's Hospital, Ludwig-Maximilians-University
Munich, Germany

Contact information of corresponding author:

Julia von Frowein, Ph.D.

Dr. von Hauner Children's Hospital, Ludwig-Maximilians-University Munich, Children's Research
Center, KUBUS KU.07, Lindwurmstrasse 2a, 80337 Munich, Germany

Tel. 0049 89 440057818

Fax. 0049 89 440057743

julia.frowein@med.uni-muenchen.de

List of abbreviations:

HB, hepatoblastoma

EFS, event-free survival

OS, overall survival

miRNAs/miRs, microRNAs

UTR, untranslated region

CD44, cluster of differentiation 44

s, standard

v, variant

Conflict of interest

The authors declare that they have no competing interests.

Financial support

This work was supported by the following foundations: Kinderkrebshilfe Ebersberg, Wilhelm Sander-Stiftung, „Mehr LEBEN für krebserkrankte Kinder – Bettina Braeu“ Stiftung and Christina Bergmann-Stiftung.

Background & Aims

MicroRNAs are important genetic regulators of physiological and pathophysiological processes including cancer initiation and progression of hepatoblastoma, the most common liver tumor in childhood. We aimed to identify malignant and metastasis promoting effects of miR-492, a miRNA we previously reported to be overexpressed in metastatic hepatoblastoma. Further, we intended to evaluate its diagnostic and prognostic potential.

Methods

Stable and transient overexpression of miR-492 in two liver tumor cell lines HepT1 and HUH7 was used to analyze features of metastatic tumor progression like proliferation, anchorage independent growth, migration and invasion. Via a mass spectrometry based proteomic screen we investigated miRNA-492 dependent effects on proteome level and explored the underlying biology. One of the predicted target genes, CD44, was experimentally validated via luciferase assays. Diagnostic and prognostic properties of miR-492 were studied in hepatoblastoma tumor samples.

Results

We show that miR-492 significantly enhances cell proliferation, anchorage independent growth, migration and invasion of hepatoblastoma cells. We also identified and validated CD44, a transmembrane adhesion receptor for hyaluronan, as direct and functional target of miR-492. This miRNA has a strong direct impact on two CD44 isoforms (standard and v10). High miR-492 expression correlates with high risk or aggressive tumors and further bears potential for predicting reduced event-free survival.

Conclusions

We identified miR-492 and its target CD44 as regulators of a number of biological features important for malignancy and metastasis. Further, we demonstrated the diagnostic and prognostic potential of miR-492, a promising novel therapeutic target and biomarker for hepatoblastoma.

Electronic

keywords: miR-492, hepatoblastoma, metastasis, CD44

Key points

- MiRNAs represent promising new targets for the development of patient-specific therapies for high risk metastatic hepatoblastoma. Here, we demonstrated that miR-492, which is significantly upregulated in metastatic hepatoblastoma, functionally triggers features of metastatic progression.
- We identified and validated two CD44 isoforms as direct targets of miR-492 and demonstrate a potential involvement in metastatic progression.
- MiR-492 expression levels correlate with current risk stratification systems for diagnostic purpose and have prognostic value. CD44 is upregulated in chemotherapeutically treated hepatoblastoma, while miR-492 expression remains stable.

This article is protected by copyright. All rights reserved.

- MiR-492 affects cancer-related pathways like multi-drug resistance and epidermal growth factor receptor-signaling.

Electronic

Introduction

Hepatoblastoma (HB) is a malignant embryonal tumor of the liver predominantly developing during early childhood.⁽¹⁾ 3-year event-free survival (EFS) of 83% and overall survival (OS) of 95% is achieved for children with standard-risk HB after pre- and postoperative cisplatin treatment combined with complete resection.⁽²⁾ For high-risk HB with metastases and /or low α -fetoprotein (AFP) levels, however, EFS and OS are still poor with rates of about 60% after intense chemotherapy and operation.^(3, 4) Aggressive HBs display biological characteristics resembling hepatic progenitor cells, like the expression of hepatic progenitor cell markers AFP, epithelial cell adhesion molecule (EpCAM) and keratin 19 (KRT19), a higher rate of proliferation and worse prognosis. In contrast, mild subtype HB cells are more differentiated (fetal), proliferate slower and display a better prognosis.⁽⁵⁾

Increasing evidence indicates that small non-coding miRNAs are important genetic regulators that critically influence cancer cell biology.^(6, 7) MiRNAs function as molecular key modulators by binding preferentially to the 3' untranslated region (3' UTR) of their target genes, resulting in messenger RNA (mRNA) decay or translational inhibition.⁽⁸⁾ All major aspects of cancer, including persistent cell proliferation, resistance to apoptosis, evasion of growth suppressors as well as the capability to migrate and invade have been linked to miRNA action.^(9, 10) Because therapeutic options are often ineffective for poor-prognosis, metastatic cancer patients,⁽⁴⁾ the development of new patient-specific approaches for cancer therapy is essential. MiRNAs represent promising new targets or might serve as therapeutic deliverable molecules.⁽¹¹⁾ Inhibition of oncogenic miRNAs and replacement of tumor-suppressor miRNAs are intensely studied strategies for future therapeutic intervention.⁽¹¹⁾ Thus it is

important to completely characterize and understand the functional role of certain miRNAs in the regulatory genetic cancer network.

Previously, we reported that the expression of miR-492 is significantly upregulated in metastatic HB and correlates highly with the expression of KRT19,⁽¹²⁾ a marker for hepatic progenitor cells as well as for cancer (initiating) stem cells,⁽¹³⁾ which have been implicated in the formation of metastases.⁽¹⁴⁾ It has further been demonstrated that miR-492 is expressed in multiple types of cancers.⁽¹⁵⁻¹⁸⁾ To better understand its contribution to the process of HB metastasis, we investigated the functional malignant role of miR-492. To investigate how miR-492 can mediate these functional alterations we aimed to identify pathways and direct target genes triggered by this miRNA. We identified cluster of differentiation 44 (CD44) as a directly regulated target gene, representing an important genetic pathway within HB metastasis. We further demonstrated the relevance and value of miR-492 as therapeutic target and biomarker for hepatoblastoma.

Material and methods

Human tumor samples

We obtained a total of 44 frozen HB tumor samples from the German liver tumor bank of the Society of Pediatric Hematology and Oncology (GPOH) in Bonn, the local tumor bank of the Department of Pediatric Surgery in Munich and hospitals in France. Tumor tissues were snap-frozen and stored in liquid nitrogen or at -80°C. Histology was evaluated by pathologists and written informed consent was obtained from each patient. The study followed the principles of the declaration of Helsinki and the study protocol was approved by the Committee of Ethics of the Ludwig-Maximilians-University in Munich (project number: 250-06). Characteristics of the patients are summarized in Supporting Table S1.

Cell lines, culture conditions and transfection

Cell lines, culture conditions and transfection methods are described in Supporting Experimental Information.

RNA isolation and reverse transcription for quantitative PCR

Total RNA (100ng-1µg) was extracted with miRNeasy Mini Kit (Qiagen, Hilden, Germany) according to the manufacturer's instructions. Quantitative gene and miRNA expression was analyzed (SsoAdvanced Universal SYBR green Supermix, Biorad, Hercules, CA, USA; TaqMan miRNA assays, Thermo Fisher Scientific, Waltham, MA, USA) on a StepOnePlus instrument (Thermo Fisher Scientific) following the manufacturer's instructions. Further details are described in Supporting Experimental Information.

Functional assays

MTT assay: Transiently transfected HepT1 and HUH7 cells were seeded in 96-well plates at a density of 5000 cells per well. Proliferation was measured by addition of MTT (final concentration 0.5mg/ml; Methylthiazolyldiphenyl-tetrazolium bromide; Sigma-Aldrich, St. Louis, MO, USA).

Cell counting: HepT1 cells stably overexpressing pMif-miR-492/pMif-control were seeded (5×10^4 cells/ml), counted microscopically every third day and reseeded.

Soft agar colony formation assay: Anchorage independent growth was analyzed via CytoSelect 96-well in vitro tumor sensitivity assays (CBA-150; Cell Biolabs, San Diego, CA, USA) following the instructions of the manufacturer.

Cell migration and invasion assay: We employed the manufacturer's instructions for CytoSelect 24-well Cell Migration and Invasion assays (Cell Biolabs) and counted invading cells under the light microscope in wet condition.

Further details of functional assays are described in Supporting Experimental Information.

Proteome Analyses via LC-MSMS

Sample preparation and mass spectrometry

Surface proteins in intact HepT1 cells stably overexpressing miR-492 were labeled with Biotin followed by cell lysis. Biotinylated and non-biotinylated proteins were purified and proteolysed with trypsin;⁽¹⁹⁾ peptides were analyzed by LC-MSMS (Orbitrap XL) and label-free quantified based on peak intensities as described elsewhere.⁽¹⁹⁾ Proteomic data was analyzed via the GenRanker module of the Genomatix Software Suite v3.7 (Genomatix Software GmbH). Further details can be found in Supporting Experimental Information.

Flow cytometry

Cells were stained with anti-rabbit CD44 (1:3000; ab157107, ABCAM, Cambridge, UK) and rabbit AlexaFluor647-conjugated secondary antibody (Cell signaling, Danvers, MA, USA) and analyzed using a LSR Fortessa flow cytometer (BD Biosciences, Franklin Lakes, NJ, USA).

Luciferase reporter assay

Luciferase constructs were generated by cloning the 3'UTR of CD44 (=CD44 v10; Ensembl transcript variant ENST0000043447), which was amplified from HepT1 cDNA using VeraSeq DNA polymerase (Biozym, Hessisch Oldendorf, Germany) into psiCHECK2 vector (Promega, Madison, WI, USA).

This article is protected by copyright. All rights reserved.

Deletion of the predicted miR-492 binding site was conducted via PCR. Dual-Luciferase Reporter Assays (Promega, Fitchburg, WI, USA) were performed in HEK-293T cells according to the manufacturer's instructions. For further details, see Supporting Experimental Information.

Statistical analyses

Experimental data are presented as mean \pm SEM (Standard Error of the Mean) of at least three independent experiments. For qPCR data the mean \pm SD (Standard Deviation) of technical triplicates is shown. Two-tailed student's t-test was used for comparison of two experimental groups, Mann-Whitney-test for the analysis of tumor samples, Fisher's Exact Test for pathway enrichment analysis, ANOVA for target prediction analysis and the log-rank (Mantel Cox) test to compare the survival distribution of two groups. P-values \leq 0.05 were considered statistically significant.

Results

MiR-492 upregulation enhances proliferation, anchorage independent growth, migration and invasion

We have previously shown that miR-492 is upregulated in metastatic HB and can be processed from the tumor marker gene KRT19.⁽¹²⁾ MiR-492 has been further reported to promote proliferation in breast and prostate cancer cells^(15, 17) and to provide the capacity of anchorage-independent growth of breast cancer cells.⁽¹⁷⁾ It remains unclear, however, whether it plays a functional role in HB tumorigenesis and metastasis. To determine its role in HB metastatic cancer progression, we examined different metastatic properties in two liver tumor cell lines HepT1 (hepatoblastoma) and HUH7 (hepatocellular carcinoma; Fig. 1; Supporting Table S2). In both cell lines, the weakest effect of miR-492 was observed on proliferation, although more visible for HepT1 (HepT1: 1.3x, 1.3x/HUH7: 1.2x; Fig. 1). Anchorage independent growth was substantially enhanced in HepT1 but only a trend

was observed in HUH7 cells (2.1x/1.5x; Fig. 1). In both cell lines, miR-492 significantly enhanced migration (1.9x/1.4x; Fig. 1). The strongest influence, however, was observed on invasion in both cell lines, which was even confirmed by stable miR-492 overexpression in HepT1 cells (2.8x, 1.9x/2.5x; Fig. 1; Supporting Fig. S1). The ability of miR-492 to alter these features of metastatic tumor progression clearly demonstrates its aggressive potential.

MiR-492 regulates oncogenic cascades to mediate metastasis

To better understand the role of miR-492 in HB, we aimed to identify distinct miR-492 induced alterations on protein level. By using an LC-MSMS (liquid chromatography – tandem mass spectrometry) based proteomic screen for comparing stably miR-492 overexpressing HepT1 cells with control cells we identified a total of 324 proteins with significantly differential abundances. While the level of 177 proteins was increased, it was decreased for 147 proteins (see Supporting Table S3). The top 50 proteins of each category are listed in Table 1. We conducted pathway enrichment analysis to gain insights into the underlying biology of differentially abundant proteins (Table 2). Concerning oncogenic progression, two important pathways were identified: First, ABC (ATP binding cassette) transporter signaling, with ABCB1, ABCC2 and ABCB11 being induced by miR-492. These ABC genes of the MDR (multidrug resistance)/TAP subfamily have been shown to transport chemotherapy substances, which may lead to multidrug resistance.⁽²⁰⁾ Second, EGFR (epidermal growth factor receptor) signaling was significantly deregulated by miR-492, which has previously been demonstrated to be involved in the autonomous growth of cancer cells.⁽²¹⁾ Both pathways suggest unfavorable progression.

Prediction and validation of direct downstream targets of miR-492

To decipher the regulatory role of miR-492 in HB and to further investigate its underlying molecular mechanism, we aimed to identify direct downstream targets of this miRNA. We determined a cut-off for significantly downregulated proteins upon miR-492 overexpression of at least 0.7 fold and performed *in silico* target prediction by TargetScan 7.0,⁽²²⁾ one of the most reliable target prediction programs.⁽²³⁾ Aiming at identifying stronger regulatory impacts, we defined a binding capability (=context++ score) of at least -0.2 as threshold level. By using this analytic strategy we identified three potential direct target genes from the list of 50 candidates, namely HSD3B1 (Hydroxy-Delta-5-Steroid Dehydrogenase, 3 Beta- and Steroid Delta-Isomerase1), SDC1 (Syndecan 1) and CD44 (cluster of differentiation 44; Table 3). SDC1 and CD44 are transmembrane glycoproteins that have been linked to cell adhesion, cell signaling and cytoskeletal organization,^(24, 25) while HSD3B1 is an enzyme, catalyzing the essential step in the formation of all classes of active steroid hormones.⁽²⁶⁾ Alterations in the abundance level of other proteins are more likely to reflect indirect effects.

CD44 exhibited the most negative total context++ score of these genes (Table 3), thus demonstrating the greatest probability for a direct miRNA-target interaction. Furthermore, an 8mer site for miR-492 binding was predicted. Because CD44 proteins have also been reported to regulate processes involved in tumor development and metastasis we focused on the CD44 - miR-492 interaction, which might explain the functional effects we observed on proliferation, anchorage independent growth, migration and invasion.

Co-transfection of HEK-293T cells with miR-492 mimics and a CD44 luciferase reporter construct induced a significant suppression of luciferase activity to 0.5 and 0.4 fold after 24h and 48h, respectively (Fig. 2A). Deletion of the predicted miR-492 binding site significantly reduced this effect (close to control levels) compared to the non-mutated construct, confirming that miR-492 directly targets the 3'UTR of CD44.

Impact of miR-492 on different splice variants of CD44

By alternative splicing, numerous CD44 transcript variants are generated (Ensembl release 85⁽²⁷⁾) from the choice of 9 variant (v) exons plus the 9 standard (s) exons.⁽²⁸⁾ Five transcripts exhibit the predicted 8mer binding site for miR-492 at position 165-172 of the respective 3'UTR: total CD44 v2-v10 (ENST00000428726), standard CD44 (CD44s;ENST00000263398), epithelial CD44 v8-v10 (ENST00000433892), CD44 v10 (ENST00000434472) and CD44 v4-v10 (XM_011520484.1⁽²⁹⁾). These isoforms contain all 9 standard exons, but differ in the composition of variant exons of the extracellular domain, suggesting that their distinct activities result from cell specific expression and the interaction with distinct ligands.

Total CD44 and epithelial CD44 could not be amplified in HepT1 cells while the existence of CD44s, CD44 v10 and CD44 v4-v10 could be confirmed by specific PCR amplification and sequencing (Fig. 2B, C; Supporting Fig. S2). These three isoforms are also expressed in HUH7 cells. Overexpression of miR-492 in HepT1 and HUH7 cells resulted in a significant downregulation of CD44s and CD44 v10 regardless of transient or stable expression (Fig. 3A). Strong transient transfection even induced a more pronounced effect on CD44 repression (24-72h after transfection) than stable overexpression and also considerably reduced the level of CD44 v4-v10 in HepT1 cells (Fig. 3A). Flow cytometric analyses of stable miR-492 expressing HepT1 cells demonstrate a global downregulation of detectable CD44 isoforms by 25% on protein level, thus confirming the observed effect (Supporting Fig. S3).

In fetal and adult liver tissue and in both cell lines CD44s was expressed strongest (mean ct-value of 24.9), followed by lower levels of CD44 v10 (mean ct-value of 31.6) and CD44 v4-v10 (mean ct-value of 34.4). During liver maturation the expression of CD44 decreases.⁽³⁰⁾ Fetal liver with undifferentiated cell types expressed highest levels of CD44 (s, v10, v4-v10), which were decreased in adult hepatocytes (Fig. 3B). Lower levels were detected in the malignant predominantly embryonal cells of HepT1, although a rather high CD44 level was expected due to their undifferentiated state.

Thus, different oncogenic factors including high miR-492 expression in malignant liver tumor cells may contribute to CD44 suppression. The embryonal/fetal liver tumor cell line HepG2⁽³¹⁾ is devoid of all 3 CD44 isoforms (data not shown⁽³²⁾).

Metastatic capacity mediated by CD44

We performed neutralizing experiments in order to evaluate the direct influence of CD44 on metastasis (Fig. 3C). Blocking CD44 resulted in a significant induction of anchorage independent growth (HepT1: 1.1x/HUH7: 1.5x), migration (1.3x/1.8x) and invasion (2.2x/1.9x) in both cell lines (Fig. 3C; Supporting Table S2; Supporting Fig. S4). Interestingly, the impact on invasion was affected strongest, resembling the effects induced by miR-492 overexpression. This observation supports the hypothesis that miR-492 induces metastatic progression of HB via CD44.

Diagnostic and prognostic value of miR-492

The diagnostic potential of pro-metastatic miR-492 in HB tumor samples (Fig. 4A,⁽¹²⁾) was evaluated by comparing its expression level in different subgroups of two HB risk stratification systems: the gene-based system (C1/C2;⁽⁵⁾; Fig. 4B) and the CHIC (Children's Hepatic tumors International Collaboration) system which is based on clinical parameters (Fig. 4C;⁽³³⁾). We observed a strong correlation of high miR-492 expression with aggressive (C2) or high risk (HR) HB subgroups.

Expression levels gradually increase from very low risk to high risk HB subgroups. For predicting the prognostic potential of miR-492 we determined the threshold level based on ROC (receiver operating characteristic) curve analysis (Fig. 4D), followed by Kaplan-Meier survival analysis (Fig. 4E). HB patients with high miR-492 expressing tumors showed a reduced event-free survival compared to patients with low miR-492 levels. This trend did, however, not reach statistical significance.

Correlation of CD44s and CD44 v10 with miR-492 expression in HB tumor samples

In order to see if the link between CD44 isoforms and miR-492 observed *in vitro* is reflected in primary HB tumor samples, miR-492, CD44s and CD44 v10 expression was analyzed via Spearman rank correlation. Unexpectedly, the analysis did not result in a significant negative correlation between miR-492 and CD44s or CD44 v10 expression (data not shown). Since another CD44 isoform (v8-v10) was recently found to confer resistance to cellular oxidative stress,⁽³⁴⁾ we investigated whether chemotherapeutical pretreatment influences CD44 or miR-492 expression in HB tumors. Interestingly, no significant difference in miR-492 expression was observed between chemotherapeutically pretreated and untreated HB tumor samples (Fig. 5A), while both CD44 isoforms were significantly upregulated in pretreated samples (Fig. 5B, C). This observation suggests that the high CD44 expression found in tumor tissue reflects the response to the chemotherapeutic pretreatment rather than the loss of the inhibitory effect of the pro-metastatic miR-492. The results furthermore define miR-492 as a stable biomarker for the indication of metastatic disease even in pretreated HB.

Discussion

MiRNAs regulate various biological processes in tumorigenesis and metastasis.⁽³⁵⁾ Although deregulation in miRNA expression is a well-known phenomenon in cancer and during metastasis, the functional role of single candidate miRNAs is still under investigation. Only few recent reports have shed light onto the functional role of miR-492 in certain types of cancers.^(15, 17, 36) In this project we investigated the functional impact of miR-492 on HB metastasis *in vitro* and deciphered the genetic cascade triggered by the miRNA. The results add to the understanding of its role in HB progression and indicate its diagnostic and prognostic relevance.

Our functional data show that miR-492 is involved in malignant processes like proliferation, anchorage independent growth, migration and most strongly in invasion, reflecting its functional

This article is protected by copyright. All rights reserved.

importance and confirming a similar function as described in other types of tumors. For breast and prostate cancer similar effects on proliferation^(15, 17) and anchorage-independent growth⁽¹⁷⁾ have been published. Strong effects based on repressing miR-492 by siRNA in liver cancer cell lines may depend on blocking miR-492 in combination with its host gene KRT19.^(12, 36) In this regard overexpression of miR-492 may deliver more specific data. According to our results, miR-492 functionally acts as pro-metastatic miRNA, which is also reflected in its high expression in aggressive or high risk HB tumors and the correlation with worse prognosis.

We identified CD44, an important transmembrane glycoprotein, as being strongly and directly regulated by miR-492. CD44 is a receptor for hyaluronan, the major component of the ECM and a co-receptor for many growth factor and cytokine signals.⁽²⁵⁾ It has been shown to modulate adhesion, cancer-cell growth, invasion, migration and metastasis.^(25, 37, 38) Therefore, CD44 provides the promise to mediate the miR-492 induced effects on proliferation, migration, invasion and anchorage independent growth. Indeed, direct impact by blocking the extracellular region of CD44 via antibody in HepT1 and HUH7 cells is discernible on anchorage independent growth, migration and most prominently on invasion.

Multiple different protein-coding isoforms are generated from the genetic region of CD44, regulating diverse oncogenic pathways with differing, even opposing functions at diverse stages of tumor progression.^(25, 37, 38) We identified a direct negative impact of miR-492 on CD44s, CD44 v10 and CD44 v4-v10.

During liver cell differentiation CD44 expression was reported to decrease,⁽³⁰⁾ which we confirmed for the specific isoforms CD44s, v10 and v4-10. Embryonal HepT1 cells, however, express even lower CD44 levels, which does not reflect their undifferentiated state, but may be explained by different oncogenic factors including the negative influence of high miR-492 expression on CD44 in malignant cells.

The positive effect of miR-492 on proliferation probably is related to the observed putatively indirect deregulation of EGFR-signaling, which has previously been demonstrated to be involved in the autonomous growth of cancer cells.⁽²¹⁾ If indeed miR-492 contributes to multidrug resistance,⁽²⁰⁾ its dangerous potential even increases.

Our results are in excellent agreement with previous investigations, which demonstrated that two different miRNAs, miR-373 and miR-520c promote tumor invasion and metastasis in breast and prostate cancer by downregulating CD44s.^(39, 40) High CD44s expression was also associated with favorable outcome in breast cancer^(41, 42) and has been described as metastasis suppressor in prostate cancer, colon cancer, colorectal cancer and neuroblastoma.⁽⁴³⁻⁴⁶⁾ These data are in line with our results as are reports that CD44 v10 has anti-metastatic competence in pancreatic cancer.⁽⁴⁷⁾ Based on these observations, we suggest that downregulation of CD44s together with CD44 v10 likely contributes to mediate the metastatic alterations observed on migration, invasion and anchorage independent growth. Although CD44 v4-v10 has been reported to be instrumental for tumor-initiation⁽⁴⁸⁾ it is expressed at extremely low level in HepT1. This observation leads us to conclude that it only slightly reduces the observed alterations, if it contributes at all.

Chemotherapy induces upregulation of CD44s and CD44 v10, but only few untreated HB tumor samples (exhibiting low miR-492 expression levels) were available for analysis. We were therefore not able to confirm the observed connections between miR-492 and CD44 in HB tumor samples. We suggest that there is an urgent need for untreated biopsy material to confirm *in vitro* observed molecular pathogenic causes of tumor development.

In summary, high miR-492 expression which we previously correlated with increased KRT19 expression in metastatic HB⁽¹²⁾ is able to trigger oncogenic functions that are essential for the development of metastases. Our results indicate that the multi-structural and multi-functional direct target gene CD44 is a regulatory link between miR-492 and oncogenic progression and provide evidence for the impact of miR-492 on metastatic HB tumor progression. These observations point to

a future therapeutic function of miR-492 as well as to its demonstrated diagnostic and prognostic value.

Acknowledgements

We thank Kristin Gammersbach and Carola Laudano for their excellent technical assistance.

References

1. Weinberg AG, Finegold MJ. Primary hepatic tumors of childhood. *HumPathol* 1983;14(6):512-37.
2. Perilongo G, Maibach R, Shafford E, et al. Cisplatin versus cisplatin plus doxorubicin for standard-risk hepatoblastoma. *NEnglJMed* 2009;361(17):1662-70.
3. Perilongo G, Shafford E, Maibach R, et al. Risk-adapted treatment for childhood hepatoblastoma. final report of the second study of the International Society of Paediatric Oncology--SIOPEL 2. *EurJCancer* 2004;40(3):411-21.
4. Zsiros J, Brugieres L, Brock P, et al. Dose-dense cisplatin-based chemotherapy and surgery for children with high-risk hepatoblastoma (SIOPEL-4): a prospective, single-arm, feasibility study. *The lancet oncology* 2013;14(9):834-42.
5. Cairo S, Armengol C, De Reynies A, et al. Hepatic stem-like phenotype and interplay of Wnt/beta-catenin and Myc signaling in aggressive childhood liver cancer. *Cancer Cell* 2008;14(6):471-84.
6. Bartel DP. MicroRNAs: target recognition and regulatory functions. *Cell* 2009;136(2):215-33.
7. Cairo S, Wang Y, De Reynies A, et al. Stem cell-like micro-RNA signature driven by Myc in aggressive liver cancer. *Proceedings of the National Academy of Sciences of the United States of America* 2010;107(47):20471-6.

8. Jonas S, Izaurralde E. Towards a molecular understanding of microRNA-mediated gene silencing. *Nature reviews Genetics* 2015;16(7):421-33.
9. Esquela-Kerscher A, Slack FJ. Oncomirs - microRNAs with a role in cancer. *NatRevCancer* 2006;6(4):259-69.
10. Suzuki HI, Katsura A, Matsuyama H, Miyazono K. MicroRNA regulons in tumor microenvironment. *Oncogene* 2015;34(24):3085-94.
11. Li Z, Rana TM. Therapeutic targeting of microRNAs: current status and future challenges. *Nature reviews Drug discovery* 2014;13(8):622-38.
12. Von Frowein J, Pagel P, Kappler R, Von Schweinitz D, Roscher A, Schmid I. MicroRNA-492 is processed from the keratin 19 gene and up-regulated in metastatic hepatoblastoma. *Hepatology* 2011;53(3):833-42.
13. Kamohara Y, Haraguchi N, Mimori K, et al. The search for cancer stem cells in hepatocellular carcinoma. *Surgery* 2008;144(2):119-24.
14. Ding SJ, Li Y, Tan YX, et al. From proteomic analysis to clinical significance: overexpression of cytokeratin 19 correlates with hepatocellular carcinoma metastasis. *MolCell Proteomics* 2004;3(1):73-81.
15. Chen Y, Zhang Z, Yang K, Du J, Xu Y, Liu S. Myeloid zinc-finger 1 (MZF-1) suppresses prostate tumor growth through enforcing ferroportin-conducted iron egress. *Oncogene* 2015;34(29):3839-47.
16. Hui AB, Lin A, Xu W, et al. Potentially prognostic miRNAs in HPV-associated oropharyngeal carcinoma. *Clinical cancer research : an official journal of the American Association for Cancer Research* 2013;19(8):2154-62.
17. Shen F, Cai WS, Feng Z, et al. MiR-492 contributes to cell proliferation and cell cycle of human breast cancer cells by suppressing SOX7 expression. *Tumour biology : the journal of the International Society for Oncodevelopmental Biology and Medicine* 2015;36(3):1913-21.
18. Zhao JJ, Yang J, Lin J, et al. Identification of miRNAs associated with tumorigenesis of retinoblastoma by miRNA microarray analysis. *Child's nervous system : ChNS : official journal of the International Society for Pediatric Neurosurgery* 2009;25(1):13-20.

19. Grosche A, Hauser A, Lepper MF, et al. The Proteome of Native Adult Muller Glial Cells From Murine Retina. *Molecular & cellular proteomics* : MCP 2016;15(2):462-80.
20. Sharom FJ. ABC multidrug transporters: structure, function and role in chemoresistance. *Pharmacogenomics* 2008;9(1):105-27.
21. Normanno N, De Luca A, Bianco C, et al. Epidermal growth factor receptor (EGFR) signaling in cancer. *Gene* 2006;366(1):2-16.
22. Agarwal V, Bell GW, Nam JW, Bartel DP. Predicting effective microRNA target sites in mammalian mRNAs. *eLife* 2015;4.
23. Fan X, Kurgan L. Comprehensive overview and assessment of computational prediction of microRNA targets in animals. *Briefings in bioinformatics* 2015;16(5):780-94.
24. Couchman JR. Syndecans: proteoglycan regulators of cell-surface microdomains? *Nature reviews Molecular cell biology* 2003;4(12):926-37.
25. Ponta H, Sherman L, Herrlich PA. CD44: from adhesion molecules to signalling regulators. *Nature reviews Molecular cell biology* 2003;4(1):33-45.
26. Simard J, Ricketts ML, Gingras S, Soucy P, Feltus FA, Melner MH. Molecular biology of the 3beta-hydroxysteroid dehydrogenase/delta5-delta4 isomerase gene family. *Endocrine reviews* 2005;26(4):525-82.
27. Kersey PJ, Allen JE, Armean I, et al. Ensembl Genomes 2016: more genomes, more complexity. *Nucleic acids research* 2016;44(D1):D574-80.
28. Schmitt M, Metzger M, Gradl D, Davidson G, Orian-Rousseau V. CD44 functions in Wnt signaling by regulating LRP6 localization and activation. *Cell death and differentiation* 2015;22(4):677-89.
29. Coordinators NR. Database Resources of the National Center for Biotechnology Information. *Nucleic acids research* 2017;45(D1):D12-D17.
30. Yovchev MI, Grozdanov PN, Joseph B, Gupta S, Dabeva MD. Novel hepatic progenitor cell surface markers in the adult rat liver. *Hepatology* 2007;45(1):139-49.

31. Lopez-Terrada D, Cheung SW, Finegold MJ, Knowles BB. Hep G2 is a hepatoblastoma-derived cell line. *Human pathology* 2009;40(10):1512-5.
32. Orian-Rousseau V, Chen L, Sleeman JP, Herrlich P, Ponta H. CD44 is required for two consecutive steps in HGF/c-Met signaling. *Genes & development* 2002;16(23):3074-86.
33. Meyers RL, Maibach R, Hiyama E, et al. Risk-stratified staging in paediatric hepatoblastoma: a unified analysis from the Children's Hepatic tumors International Collaboration. *The lancet oncology* 2017;18(1):122-31.
34. Ishimoto T, Nagano O, Yae T, et al. CD44 variant regulates redox status in cancer cells by stabilizing the xCT subunit of system xc(-) and thereby promotes tumor growth. *Cancer Cell* 2011;19(3):387-400.
35. Pencheva N, Tavazoie SF. Control of metastatic progression by microRNA regulatory networks. *Nature cell biology* 2013;15(6):546-54.
36. Jiang J, Zhang Y, Yu C, Li Z, Pan Y, Sun C. MicroRNA-492 expression promotes the progression of hepatic cancer by targeting PTEN. *Cancer cell international* 2014;14(1):95.
37. Louderbough JM, Schroeder JA. Understanding the dual nature of CD44 in breast cancer progression. *Molecular cancer research : MCR* 2011;9(12):1573-86.
38. Zoller M. CD44: can a cancer-initiating cell profit from an abundantly expressed molecule? *Nature reviews Cancer* 2011;11(4):254-67.
39. Huang Q, Gumireddy K, Schrier M, et al. The microRNAs miR-373 and miR-520c promote tumour invasion and metastasis. *Nature cell biology* 2008;10(2):202-10.
40. Iczkowski KA. Cell adhesion molecule CD44: its functional roles in prostate cancer. *American journal of translational research* 2010;3(1):1-7.
41. Berner HS, Suo Z, Risberg B, Villman K, Karlsson MG, Nesland JM. Clinicopathological associations of CD44 mRNA and protein expression in primary breast carcinomas. *Histopathology* 2003;42(6):546-54.

42. Diaz LK, Zhou X, Wright ET, et al. CD44 expression is associated with increased survival in node-negative invasive breast carcinoma. *Clinical cancer research : an official journal of the American Association for Cancer Research* 2005;11(9):3309-14.
43. Choi SH, Takahashi K, Eto H, Yoon SS, Tanabe KK. CD44s expression in human colon carcinomas influences growth of liver metastases. *International journal of cancer Journal international du cancer* 2000;85(4):523-6.
44. Jaeger EB, Samant RS, Rinker-Schaeffer CW. Metastasis suppression in prostate cancer. *Cancer metastasis reviews* 2001;20(3-4):279-86.
45. Pereira PA, Rubenthiran U, Kaneko M, Jothy S, Smith AJ. CD44s expression mitigates the phenotype of human colorectal cancer hepatic metastases. *Anticancer research* 2001;21(4A):2713-7.
46. Shtivelman E, Bishop JM. Expression of CD44 is repressed in neuroblastoma cells. *Molecular and cellular biology* 1991;11(11):5446-53.
47. Navaglia F, Fogar P, Greco E, et al. CD44v10: an antimetastatic membrane glycoprotein for pancreatic cancer. *The International journal of biological markers* 2003;18(2):130-8.
48. Zeilstra J, Joosten SP, Van Andel H, et al. Stem cell CD44v isoforms promote intestinal cancer formation in *Apc(min)* mice downstream of Wnt signaling. *Oncogene* 2014;33(5):665-70.

Table 1. Top 50 proteins up- and downregulated by miR-492

Top 50 proteins upregulated by miR-492			Top 50 proteins downregulated by miR-492		
Gene symbol	Anova (p)	fold change miR-492/control	Gene symbol	Anova (p)	fold change miR-492/control
CALML5	0.0248	300.66	GTF2F1	0.0046	0.28
KRT16	0.0193	9.56	SNRPC	0.0470	0.33
PTGFRN	0.0002	4.76	GTF2F2	0.0002	0.33
SLC26A2	0.0226	4.41	SERPINI1	0.0176	0.35
SLC1A3	0.0012	3.17	MTTP	0.0004	0.36
SLC27A2	0.0265	2.77	AMBP	0.0193	0.40
HSPA8	0.0042	2.67	PALLD	0.0133	0.42
ABCB11	0.0001	2.61	AHSG	0.0006	0.43
DPEP1	0.0065	2.45	MYADM	0.0341	0.44
IGSF1	0.0000	2.37	CD74	0.0036	0.46
TBC1D4	0.0041	2.34	AFP	0.0034	0.46
LMCD1	0.0168	2.25	AFG3L2	0.0011	0.47
DUOXA1	0.0001	2.15	ANPEP	0.0056	0.48
PTPN23	0.0024	2.05	AHSG	0.0033	0.48
METTL7B	0.0071	1.93	EPPK1	0.0004	0.49
HSPG2	0.0064	1.92	CDC20	0.0446	0.49
ACSS3	0.0005	1.82	LIN28B	0.0419	0.51
SYT2	0.0013	1.80	FBLN1	0.0074	0.51
PTPN6	0.0184	1.80	HSD3B1	0.0074	0.51
FGA	0.0004	1.78	VSIG10L	0.0154	0.51
TST	0.0503	1.78	TAGLN2	0.0237	0.52
SLC19A3	0.0278	1.76	ICAM1	0.0044	0.52
LIN7A	0.0065	1.74	PVRL3	0.0123	0.56
PELP1	0.0334	1.73	HMGB1	0.0083	0.56
NIPSNAP1	0.0005	1.73	PTPRM	0.0485	0.56
DTD1	0.0052	1.72	ABCG2	0.0005	0.56
MAOB	0.0013	1.72	TUBB6	0.0223	0.56
SUGP2	0.0456	1.72	FKBP3	0.0289	0.57
EPCAM	0.0059	1.69	VIL1	0.0000	0.57
APOBEC3C	0.0219	1.69	VCAN	0.0385	0.58
PROM1	0.0028	1.65	SDC1	0.0074	0.58
PODXL	0.0007	1.64	FLNB	0.0104	0.58
MTHFS	0.0261	1.63	FAM160B1	0.0474	0.58
TBC1D24	0.0085	1.62	NEU1	0.0135	0.59
SLC12A2	0.0010	1.62	TXNRD1	0.0101	0.60
LMNB1	0.0178	1.61	SERPINB1	0.0020	0.60
H2AFY	0.0230	1.59	EXOSC5	0.0447	0.60
AKR1B1	0.0000	1.59	GORASP2	0.0477	0.61
ALDH1A3	0.0208	1.58	GTF2H2	0.0002	0.61
FAHD2A	0.0352	1.58	AACS	0.0199	0.61
AKR1B10	0.0080	1.58	PPM1G	0.0363	0.62
PNP	0.0002	1.57	ALB	0.0175	0.62
CPPED1	0.0085	1.56	UBAP2	0.0449	0.63
ZBED9	0.0208	1.56	TUBB2B	0.0012	0.63
CA13	0.0102	1.56	DDX55	0.0011	0.63

ACOT13	0.0162	1.54		KPNA3	0.0023	0.64
MAP1A	0.0143	1.54		CD44	0.0152	0.64
PCCA	0.0101	1.53		CTSB	0.0355	0.64
BAIAP2L1	0.0136	1.52		TMPO	0.0064	0.65
FLOT1	0.0024	1.50		ANXA3	0.0252	0.65

Top 50 proteins ($p < 0.05$ of Anova analysis) are sorted according to fold induction/reduction (fold change) in stable miR-492 overexpressing HepT1 cells compared to control cells that stably express a construct lacking the miR-492 sequence.

Table 2. Signal transduction pathways overrepresented by proteins

Pathway	P-value	# Proteins (observed)	# Proteins (expected)	# Proteins (total)	List of observed proteins
ATP BINDING CASSETTE, SUBFAMILY G (WHITE)	1.87E-07	10	1.1	81	EPCAM, ABCC2, ABCG2, JAG1, XPC, TAGLN2, CD44, PROM1, ABCB1, AHR
EPIDERMAL GROWTH FACTOR RECEPTOR	3.68E-05	18	6.1	432	PTPN23, KRT16, EPCAM, ROR1, ABCG2, IGF1R, SLC12A2, AGK, VCAN, CMBL, DNAJA3, ANXA6, SCAMP3, FLOT1, MAP1A, CD44, AKR1B10, NEU1
REDOX	1.73E-04	12	3.4	244	GGT1, AKR1B1, ABCC2, GPT2, PPIC, GLRX3, SORD, ICAM1, FDXR, H2AFY, TXNRD1, ALB
HYPOXIA INDUCIBLE FACTOR 1, ALPHA SUBUNIT (BASIC HELIX LOOP HELIX TRANSCRIPTION FACTOR)	2.81E-04	11	3.1	220	IDH1, TYMS, SLC12A2, SLC19A3, ANXA3, SORD, TXNRD1, CD74, PROM1, ABCB1, AHR
MATRIX METALLOPROTEINASE	3.00E-03	11	4.1	294	EPCAM, STOML2, HMGB1, FBLN1, GOLPH3, ANPEP, CTSB, FLOT1, CNN2, CD44, NEU1
ENDOCYTIC	3.66E-03	13	5.5	392	SDC1, PRNP, RAB8A, LIN7A, HSPA8, ASGR1, SYT2, ANPEP, ANXA6, FLOT1, MAP1A, CD44, ALB
NUCLEAR RECEPTOR SUBFAMILY 1, GROUP I, MEMBER 2	3.94E-03	4	0.7	46	SCD, AKR1B10, ABCB1, AHR
HEPATOCTE GROWTH FACTOR RECEPTOR	5.05E-03	6	1.6	112	SDC1, EPCAM, IGF1R, ELAVL1, CD44, CD74
ATP BINDING CASSETTE, SUBFAMILY C (CFTR/MRP)	6.32E-03	5	1.2	83	ABCB11, ABCC2, ABCG2, SULT2A1, ABCB1
ATP BINDING CASSETTE, SUBFAMILY B (MDR/TAP)	6.49E-03	6	1.7	118	ABCB11, ALDH1A3, ABCC2, ABCG2, PROM1, ABCB1
CD36 MOLECULE (THROMBOSPONDIN RECEPTOR)	7.70E-03	5	1.2	87	AHSG, SCD, KIAA0020, MTPP, TBC1D4
CYSTIC FIBROSIS TRANSMEMBRANE CONDUCTANCE REGULATOR (ATP BINDING CASSETTE SUBFAMILY C, MEMBER 7)	9.00E-03	4	0.8	58	HSPA8, SLC12A2, AHCYL1, ADK

Pathway enrichment analysis. Proteins with increased abundance in miRNA-492 overexpressing cells (bold; List of observed proteins) and decreased abundance (italics) that belong to different signal transduction pathways (Pathways) significantly overrepresented (P-value; Fisher's Exact Test) in the dataset, calculated based on the number of proteins identified from respective pathways [# Proteins

(observed)] and the number of expected proteins from a random dataset [# Proteins (expected)].

Pathways are sorted by significance.

Table 3. Prediction of direct miR-492 targets

Gene symbol	Anova (p)	fold change miR-492/ control	total context++ score	predicted miR-492 binding site
HSD3B1	0.0074	0.51	-0.27	7mer
SDC1	0.0074	0.58	-0.30	8mer
CD44	0.0152	0.64	-0.67	8mer

Significant negatively regulated proteins of at least 0.7 fold compared to control cells upon stable miR-492 overexpression were screened for their potential of being direct targets of miR-492. By using TargetScan 7.0, we determined the total context++ scores and the length of the predicted binding site. Genes with total context++ scores of at least -0.2 were defined as potent candidates and are shown here.

Figure Legends

Fig. 1. Functional influence of miR-492. The influence of miR-492 on proliferation measured via MTT (transient, serum-deprived) and cell counts (stable), anchorage independent growth (AIG), migration and invasion compared to control cells in HepT1 and HUH7 cells is depicted. Overexpression of miR-492 slightly enhanced proliferation (HepT1-stable: n=10 splitting events; HepT1-transient: n=4; HUH7-transient: n=3; 6 wells/exp; ns, not significant) and increased the ability of anchorage independent growth (HepT1-stable: n=3; 9 wells/exp.; #, each exp. significant; HUH7-transient: n=3; 4 wells/exp.; 2 of 3 exp. significant). Migration (HepT1-stable: n=3; 2 wells/exp.; HUH7-transient: n=3; 1 well/exp.) and invasion (HepT1-stable: n=4; 1 well/exp.; HepT1-transient: n=3; 1-2 wells/exp.; HUH7-transient: n=3; 1well/exp.) were significantly enhanced by miR-492 overexpression. Mean values \pm SEM of replicate experiments are indicated. * $p \leq 0.05$, ** $p \leq 0.01$ of two-tailed t-test. Fc \pm SEM values and p-values are listed in Supporting Table S2.

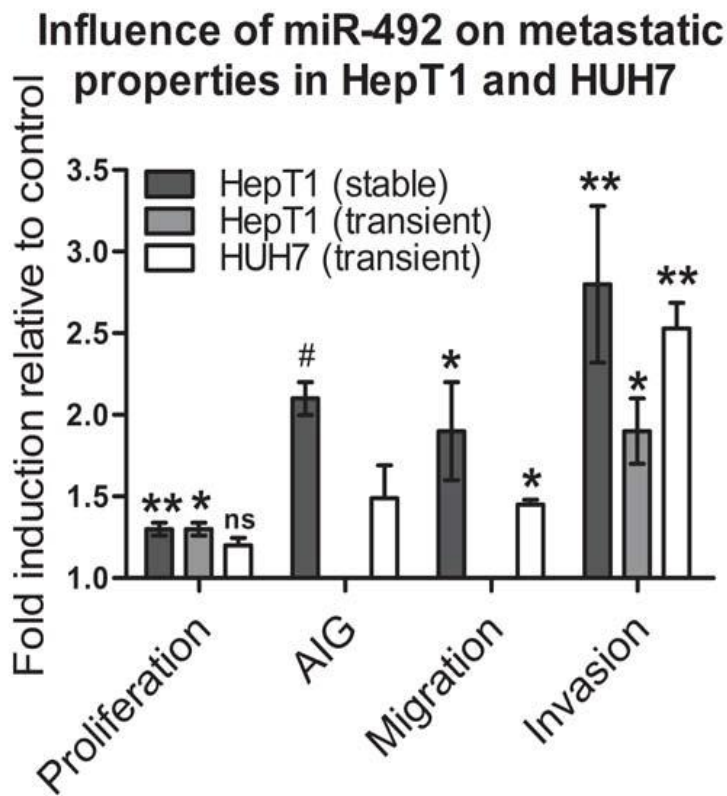
Fig. 2. MiR-492 interacting with CD44 3'UTR. (A) A direct interaction of miR-492 mimic with the 3'UTR of CD44 is demonstrated by a strong reduction of luciferase activity in HEK-293T cells (n=3), while deletion (del) of the predicted binding site (position 165-172 of CD44 v10 3'UTR; ENST00000434472) resulted in a significant reduction of this effect (n=3). Data of 24h (dark grey) and 48h (white) are depicted. Columns represent the mean \pm SEM relative to respective controls. * $p \leq 0.05$, ** $p \leq 0.01$ of two-tailed t-test. (B) Schematic overview of CD44 isoforms with predicted 8mer binding sites for miR-492 in their 3'UTRs (CD44 standard, CD44 v10 and CD44 v4-v10). Standard exon 9 is spliced out in most CD44 isoforms⁽²⁸⁾ and therefore not included in our schematic overview. (C) Summary table including the size of CD44 isoforms expressed in HepT1 cells. Gene transcripts as depicted in Ensembl Genomes or from NCBI.

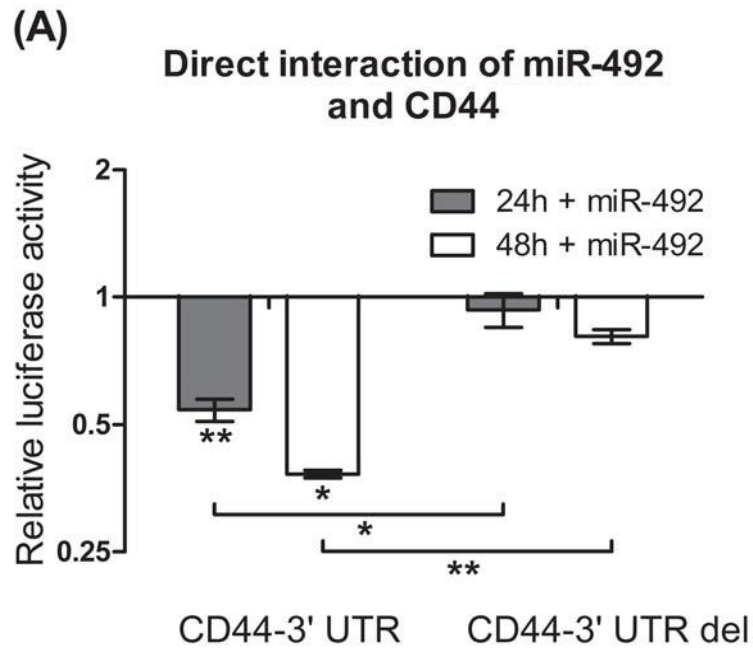
Fig. 3. (A) Downregulation of different CD44 isoforms by miR-492. The influence of miR-492 on CD44s, CD44 v10 and CD44 v4-v10 was determined by qPCR. MiR-492 was stably (pMif-miR-492/-control) or transiently (miR-492 mimics/control mimics) overexpressed in HepT1 and HUH7 cells. Columns represent the mean \pm SEM of stable miR-492 expressing cells (n=3-4) or mimic experiments (n=3-7). * $p \leq 0.05$, ** $p \leq 0.01$ of two-tailed t-test using Δ ct- (cycle-threshold) values; ns, not significant; na, not analyzed. (B) Fold change expression of CD44s, CD44 v10 and CD44 v4-v10 in well-differentiated HUH7 cells, fetal and adult liver tissue is depicted relative to the level in embryonal HepT1 cells. Error bars indicate the SD of triplicates; nd, not detectable. (C) The metastatic capacity (proliferation; anchorage independent growth, AIG; migration; invasion) of HepT1 and HUH7 cells treated with a CD44-blocking antibody (Hermes-1; 10 μ g/ml; n=3-6) was compared to isotype specific control treatment. Mean values \pm SEM are indicated. * $p \leq 0.05$, ** $p \leq 0.01$, *** $p \leq 0.001$ of two-tailed t-test. Fc \pm SEM values and p-values are listed in Supporting Table S2.

Fig. 4. Diagnostic and prognostic value of miR-492. Differential expression of miR-492 in tumor tissue of HB patients analyzed via qPCR: (A) Non-metastatic versus metastatic HB tissue, (B) mild C1 versus aggressive C2 tumors and (C) different CHIC (Children's Hepatic tumors International Collaboration) risk groups. Y axis represents relative expression normalized to adult liver tissue. VLR, very low risk; LR, low risk; IR, intermediate risk; HR, high risk. Horizontal lines in dot blots denote means with SEM. * $p \leq 0.05$, ** $p \leq 0.01$ of Mann-Whitney test. (D) Receiver-operating characteristic (ROC) curve analysis of miR-492 expression for discriminating metastatic from non-metastatic patients. AUC, area under the curve. The value of 1.4 was determined as threshold level for miR-492 expression (log₂ fold change expression compared to adult liver tissue) to best separate metastatic from non-metastatic tissue. (E) Kaplan-Meier curve for depicting event-free survival of patients with HB when classified according to high miR-492 ($x > 1.4$) and low miR-492 ($x < 1.4$) expression. P-value of Log-rank (Mantel-Cox) test.

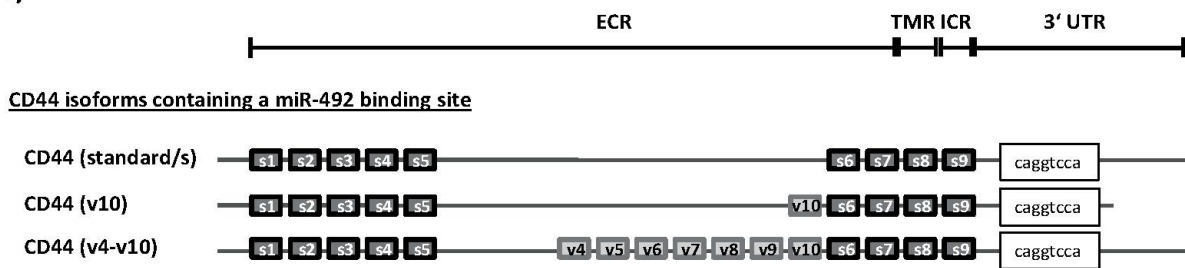
Fig. 5. Influence of chemotherapy on miR-492, CD44s and CD44 v10 expression in HB tumor samples.

MiR-492 (A), CD44s (B) and CD44 v10 (C) expression between untreated and chemotherapeutically pretreated tumors was compared. Means \pm SEM of expression data including 44 (A), 36 (B), 35 (C) HB tumor samples are indicated. ns, not significant; ** $p \leq 0.01$ of Mann-Whitney test.





(B)



(c)

CD44 transcript variant	transcript length	number of exons	position of miR-492 binding site in 3'UTR	length of 3'UTR	transcript ID
standard	4589bp	9 exons	165-172	3069 bp	ENST00000263398
v10	1634bp	10 exons	165-172	333 bp	ENST00000434472
v4-v10	5204 bp	16 exons	165-172	3069 bp	XM_011520484.1

ECR = extracellular region
ICR = intracellular region
TMR = transmembrane region
s1-s9 = standard exons
v4-v10 = variable exons
caggtcca = miR-492 binding site

